Theory and simulation of rotational shear stabilization of turbulence

Cite as: Physics of Plasmas **5**, 1784 (1998); https://doi.org/10.1063/1.872847
Submitted: 17 November 1997 • Accepted: 29 January 1998 • Published Online: 27 April 1998

R. E. Waltz, R. L. Dewar and X. Garbet

Theory and simulation of rotational shear stabilization of turbulence*

R. E. Waltz,† R. L. Dewar,[a] and X. Garbet[b]
General Atomics, P.O. Box 85608, San Diego, California 92186-5608

(Received 17 November 1997; accepted 29 January 1998)

Numerical simulations of ion temperature gradient (ITG) mode transport with gyrofluid flux tube codes first lead to the rule that the turbulence is quenched when the critical $E\times B$ rotational shear rate γ_{E_crit} exceeds the maximum of ballooning mode growth rates γ_0 without $E\times B$ shear [Waltz, Kerbel, and Milovich, Phys. Plasmas **1**, 2229 (1994)]. The present work revisits the flux tube simulations reformulated in terms of Floquet ballooning modes which convect in the ballooning mode angle. This new formulation avoids linearly unstable ''box modes'' from discretizing in the ballooning angle and illustrates the true nonlinear nature of the stabilization in toroidal geometry. The linear eigenmodes can be linearly stable at small $E\times B$ shear rates, yet Floquet mode convective amplification allows turbulence to persist unless the critical shear rate is exceeded. The flux tube simulations and the $\gamma_{E\_\mathrm{crit}}\approx\gamma_0$ quench rule are valid only at vanishing relative gyroradius. Modifications and limits of validity on the quench rule are suggested from analyzing the finite relative gyroradius ''ballooning-Schrödinger equation'' [R. L. Dewar, Plasma Phys. Controlled Fusion **39**, 437 (1997)], which treats general ''profile shear'' (x variation in γ_0) and ''profile curvature'' (x^2 profile variation). © *1998 American Institute of Physics.*
[S1070-664X(98)94505-0]

I. INTRODUCTION

Stabilization of turbulence in tokamaks by the equilibrium $E\times B$ rotational shear is now thought to be a key mechanism leading to both H (high)-mode edge and core transport barriers.[1] Early papers based on nonlinear two-point renormalization theories by Biglari, Diamond, and Terry (BDT)[2] and others[3,4] suggested that turbulence would be suppressed when the $E\times B$ rotational shear rate γ_E became comparable to $\Delta\omega(\Delta k_x/\Delta k_y)$ where $\Delta\omega$ is a turbulence decorrelation rate used interchangeably in the theory with $D\Delta k_x^2$ where D is a turbulent diffusivity, and Δk_x and Δk_y are radial and poloidal inverse turbulence correlation lengths. Other work by Connor, Taylor, and Wilson (CTW)[5,6] suggested that if turbulence followed linear eigenmode stability, then even vanishing small $E\times B$ shear rates would reduce toroidal transport driven by strongly unstable ballooning modes to small levels expected of ''slab'' geometry. In contrast, numerical simulations of ion temperature gradient (ITG) mode transport with gyrofluid flux tube codes first lead to the approximate rule that turbulence is not just suppressed but quenched when the critical $E\times B$ rotational shear rate $\gamma_E=(r/q)\partial(q\nu_{E\times B}/r)/\partial r$ exceeded $\gamma_{\max}$ the maximum of ballooning mode growth rates γ_0 in the absence of the $E\times B$ shear.[7,8] This approximate but quantitative quench rule $\gamma_{E-\mathrm{crit}}\approx\gamma_{\max}$ has been incorporated in recent toroidal transport models as a quenching factor $(1-\gamma_E/\gamma_{\max})$ on diffusion; such models have had some success in describing core transport barriers.[9]

The referenced theories[2–6] as well as the flux tube simulations[7,8] are taken in the limit of vanishing relative gyroradius ($\rho_*\to 0$). Even in this simple limit in which the $E\times B$ velocity greatly exceeds the diamagnetic velocity, only the equilibrium $E\times B$ is allowed a radial x variation or ''profile shear,'' and x^2 variations or ''profile curvature'' is ignored, the physical mechanism for $E\times B$ rotational shear stabilization in toroidal geometry and its proper numerical simulation can be quite subtle. For tokamak geometry in the $\rho_*\to 0$, or high-n (toroidal mode number) limit, the standard ballooning mode representation[10] describes eigenmodes when their is no profile variation of the plasma gradients and only shear in the magnetic field line pitch $\hat{s}=d\ \ln q/d\ln r$. In the presence of $E\times B$ rotational shear, there are two pictures: for a given n, unstable ballooning modes at outboard poloidal ballooning angles θ_0 near 0 are linearly coupled to typically stable inboard modes (θ_0 near π) by the differential operation $\partial/\partial t+(\gamma_E/\hat{s})\partial\theta_0$, i.e., θ_0 is no longer a ''good quantum number.'' Equivalently ballooning modes at a given θ_0 begin to rotate or convect in the ballooning angle[11–13] $\theta_0\to\theta_0+(\gamma_E/\hat{s})t$ and pass alternately between unstable outboard angles and stable inboard angles. CTW formally showed[5,6] that even at small shear rates γ_E drift-ballooning modes eigenmodes would acquire the time average growth rate $\langle\gamma\rangle_0=\oint\gamma_0(\theta_0)d\theta_0/2\pi$, where $\gamma_0(\theta_0)$ are the ballooning mode rates at $\gamma_E=0$. We refer to this as the CTW linear circulation rule or angle average rate. It is also implicit in Ref. 13. These angle average rates will tend to be at low slab-like levels and can be stable $\langle\gamma\rangle_0<0$ even when some ballooning mode rates are unstable $\gamma_0(\theta_0)>0$.

The first nonlinear ballooning modes simulations[7,8] showed that for cases at small γ_E where $\langle\gamma\rangle_0<0$, the turbulence persisted at only slightly reduced levels. However, it

*Paper kWeaI1-5 Bull. Am. Phys. Soc. **42**, 1946 (1997).
†Invited speaker.
[a]The Australian National University.
[b]Association Euratom-CEA Cadarache.

was subsequently realized that because the simulation code treated θ_0 as a discrete variable (corresponding to a flux tube of finite radial width) and $E\times B$ shear as a linear mode coupling mechanism, the numerical system could be subject to unstable ''box modes.'' [14] Indeed, that proved to be the case. Even when the system should have been stable by the CTW circulation rule, it contained a linearly growing oscillation which could be interpreted as an unphysical ''box mode'' and was found to be stabilized at the quench point. This cast doubt on the $\gamma_{E\_\mathrm{crit}}\approx\gamma_{\max}$ quench rule and reopened the question: Is the $E\times B$ shear rate required for linear eigenmode stability[5,6] a better guide?

In this paper, we revisit the flux tube ITG simulations but with a revised numerical method which first treats θ_0 as a continuous variable (infinite radial box) going to a novel ''mode-centered Floquet ballooning mode representation'' and then passing to discrete θ_0 in treating the nonlinear coupling. The new representation given in Sec. II of the paper explicitly recovers the CTW angle average linear eigenmodes at small γ_E. A further benefit of the new representation is that it explicitly displays a term $(\gamma_E/\hat{s})\partial/\partial\theta$ which can be associated with the ''poloidal breakup effect'' which acts in both cylindrical (''slab'') and toroidal geometry. A ballooning mode can be thought of as a fixed ballooning angle phasing $[\exp(i\theta_0)]$ between neighboring poloidal harmonics m and $m\pm1$. At low levels, $E\times B$ shear first breaks up this phasing, but at very high levels it breaks up the poloidal harmonics themselves. Thus even if the weak shear (small γ_E) CTW circulation rule eigenmodes are unable $\langle\gamma\rangle_0>0$, the true eigenmode (time average) rates $\langle\gamma\rangle$ will vanish at large enough γ_E.

In toroidal geometry ITG simulations with the new nonlinear Floquet ballooning mode representation, although different in quantitative detail, again recover an approximate quench rule $\gamma_{E\_\mathrm{crit}}\approx\gamma_{\max}$ over a substantial range of parameters including low values of magnetic shear $\hat{s}$. The new simulations illustrated in Sec. III clearly show that the critical $E\times B$ shear rate does not follow the shear rate required for eigenmode stability $\langle\gamma\rangle=0$. Even when the eigenmodes are stable, at sufficient levels of turbulence the Floquet ballooning modes can obtain sufficient convective amplification in rotating through the bad curvature to nonlinear pass turbulent energy to convectively decaying modes passing through good curvature. The quench results when the $E\times B$ shear rotation rate $\gamma_E/\hat{s}$ is too fast for this process. In contrast, and in contradiction to the nonlinear renormalization theories[2–4] which do not distinguish between slab and toroidal geometry, simulations in slab geometry do, in fact, follow eigenmode stability at both small and large γ_E with γ_{E_crit} much larger than $\gamma_{\max}$. Thus the quench rule $\gamma_{E\_\mathrm{crit}}\approx\gamma_{\max}$ obtained in the limit of vanishing ρ_* is intended only to describe toroidal geometry and it is not associated with linear eigenmode stability in any simple way. Furthermore, we will show that while in some instances the quench rate can be associated with the $E\times B$ shear rate for a given level of linear connective amplification this is not a general guide.

While it should be cautioned that $\gamma_{E\_\mathrm{crit}}\approx\gamma_{\max}$ is an approximate rule for toroidal geometry and may require modification when more physics is added to the ITG formulation with adiabatic electrons, we believe $E\times B$ profile shear stabilization in the vanishing ρ_* limit is now well understood. However, real tokamak plasmas exist at small but finite ρ_* (and the effective ρ_* in an edge plasma may not be small). Where and how the $\gamma_{E\_\mathrm{crit}}\approx\gamma_{\max}$ rule breaks down or should be modified for general plasma profiles is not easy to assess. Despite the fact that this paper shows that nonlinear simulations in the vanishing ρ_* limit need not respect global eigenmode stability, our first attempt to consider general profile shear and profile curvature looks to general global eigenmode stability as a guide. In Sec. IV, we recast and generalize the work of Dewar[15] and others.[16] These formulations start with the ansatz that complex growth rate of high-n ballooning modes at radial location r, $\gamma_0(\theta_0,r)$, can be approximated in its θ_0 dependence as an approximate linear function of $\cos(\theta_0)$. (Re γ_0 correspond to the growth rate and Im γ_0 to the frequency.) Then the dependence of $\gamma_0(\theta,r)$ on r is Taylor expanded in $x=r-r_0$. This results in a ''ballooning-Schrödinger'' dispersion relation[15] dependent on general profile shear $\gamma_0'=d\gamma_0/dx$ and profile curvature $\gamma_0''=d^2\gamma_0/dx^2$. In the limit of $\rho_*\to0$, $\mathrm{Im}(\gamma_0')/k_y=\gamma_{\mathrm{mode}}\to\gamma_E$ as it results from the shear in the $E\times B$ Doppler shift velocity. This suggests the obvious first generalization of the rule $\gamma_{E\_\mathrm{crit}}\approx\gamma_{\max}$, when the $E\times B$ velocity is comparable to the diamagnetic level intrinsic mode velocities, is to hypothesize that $\gamma_{\mathrm{mode}}=(r/q)\partial(q\nu_{\mathrm{mode}}/r)/\partial r$ where ν_{mode} is the total mode phase velocity of the mode with maximum growth rate (not just the $E\times B$ velocity as in the definition of γ_E) which must exceed $\gamma_{\max}\{=\max[\gamma_0(\theta_0,r_0)]\}$ to quench the turbulence. Solution of the ballooning-Schrödinger dispersion relation may furthermore suggest a criterion for ignoring the effects of profiles curvature. The eigenmode solutions are of two types: ''bound'' and ''passing.'' For sufficiently weak profile shear γ_0' or strong profiles curvature γ_0'', the solutions are bound. However, for sufficiently large profile shear, the bound solutions ''jump'' to the passing solutions which are independent of profile curvature and recover the CTW circulation rule rate (again without the poloidal breakup effect also missing from the ballooning-Schrödinger equation). It seems reasonable to suggest that the revised quench rule $\gamma_{\mathrm{mode}}>\gamma_{\max}$ is unlikely to hold unless γ_{mode} is sufficiently large that the ballooning-Schrödinger eigenmodes are past the jump condition. In Sec. IV we show how to evaluate this hypothetical validity condition. We also give a short discussion on the difficulties of testing this hypothesis in full radius nonlinear simulations. Section V summarizes our main conclusions.

II. FORMULATION OF THE NONLINEAR FLOQUET BALLOONING MODE REPRESENTATION

We proceed from the nonlinear ballooning mode representation of the gyro-Landau fluid equation for the ITG mode turbulence of Ref. 7 written here in schematic form:

$$dF/dt=(\gamma_E/\hat{s})\partial F/\partial\theta_0+L[\theta-\theta_0,\cos(\theta),\partial/\partial\theta]F, \quad (1)$$

where $dF/dt=\partial F/\partial t+\tilde{\nu}_E\cdot\nabla F$ represents the nonlinear $E\times B$ convective time derivative for a general fluid moment

$F_{ky}(\theta,\theta_0)$. $k_y = nq/r$, θ is the usual extended poloidal angle, and θ_0 is the ballooning mode angle related to the radial wave number label by $k_x' = k_y \hat{s}\theta_0$. L is a linear operator in which the $\cos(\theta)$ dependence represents the toroidal curvature terms. We first treat the $E\times B$ shear term with γ_E as a convection in θ_0 by the transformation[11,13] $t = t'$ and $\theta_0 = \theta_0' - \gamma_E/\hat{s}t'$, followed by the rotating frame transformation $\theta = \theta' - \gamma_E/\hat{s}t'$. The combined transformation leaves the physical radial wave number $k_x = k_y\hat{s}(\theta_0 - \theta)$ and the nonlinear coupling invariant. Dropping the prime notation the transformed equation becomes

$$dF/dt = -(\gamma_E/\hat{s})\partial F/\partial\theta + L[\theta-\theta_0, \cos(\theta-\gamma_E/\hat{s}t), \partial/\partial\theta]F. \quad (2)$$

By discretizing Eq. (2) rather than Eq. (1), we avoid ''box mode'' instabilities[14] and arrive at a true infinite-n ballooning mode representation. However, now $F_{ky}(\theta,\theta_0)$ represents a ''Floquet ballooning mode'' since the coefficients of the linear operation associated with the toroidal curvature now has a cyclic time dependence. The linear modes at a given k_y (or n) have instantaneous growth rates $\partial \ln F/\partial t$ which cycle in time with the period $2\pi/(\gamma_E/\hat{s})$ with θ_0 becoming a degenerate label denoting only the phase of the cycle. As $\cos(\theta-\gamma_E/\hat{s}t)$ cycles near $1(-1)$ corresponding to bad (good) curvature, the modes will have their highest (lowest) instantaneous growth. At low γ_E, the cycling is very slow and it is not surprising that we recover the time average growth rate or eigenmode rates by the CTW[5] circulation rule $\langle\gamma\rangle_0 = \oint \gamma_0(\theta_0)d\theta_0/2\pi$, where $\gamma_0(\theta_0)$ are the ballooning mode rates at $\gamma_E = 0$. However, at larger γ_E, the $(\gamma_E/\hat{s})\partial F/\partial\theta$ term, which we have called the poloidal breakup effect, distorts the $\gamma_E = 0$ wave functions and the time average rate becomes less than $\langle\gamma\rangle_0$ invariably becoming stable at $\gamma_{E\_\langle\gamma\rangle}$. Although not explicitly verified by us, it is likely that the true time average rate is given by $\langle\gamma\rangle = \oint\gamma(\theta_0)d\theta_0/2\pi$, where $\gamma(\theta_0)$ are the eigenmodes of Eq. (2) with the time dependence of $\cos(\theta-\gamma_E/\hat{s}t)$ suppressed. In fact, it is useful to define the poloidal breakup rate γ_{E_PB} as the level of γ_E required to stabilize $\gamma(\theta_0)$ at the most unstable θ_0.

III. NUMERICAL ILLUSTRATION SUPPORTING THE $\gamma_{E\_\mathrm{crit}} \approx \gamma_{\max}$ TOROIDAL RULE

In this section, we proceed to illustrate that $\gamma_{E\_\mathrm{crit}} \approx \gamma_{\max}$ is a good approximate rule for quenching turbulence in toroidal geometry with variations on the standard case of ITG turbulence with adiabatic electrons from Refs. 7 and 8. In the notation of that reference $R/a = 3$, $a/L_T = 3$, $a/L_n = 1$, $\hat{s} = 1$, $q = 2$, $T_i/T_e = 1$, and local shear or Shafranov shift $\alpha = 0$. In the absence of equilibrium rotational shear, the present formulations and results remain unchanged. We direct the reader to Refs. 7 and 8 and references therein for a discussion on the general saturation mechanism from the nonlinearly driven $E\times B$ flow shears or $n=0$ ''radial modes.'' We stress at the outset that the parallel velocity shear rate γ_P drives the ITG mode much in the same way that the temperature gradient parameter a/L_T drives the modes[17] and it causes the maximum ballooning modes rate $\gamma_{\max}$ to increase roughly with γ_P^2. For purely toroidal rotation, γ_P and γ_E are related by $\gamma_P = (Rq/r)\gamma_E$ and depending on (Rq/r), $\gamma_{\max}$ driven by γ_P may keep $\gamma_{\max}$ larger than γ_E for increasing γ_E avoiding quench as illustrated in Ref. 7. However, in these illustrations, we artificially take only $\gamma_P = 0$ and assume finite γ_P is to be included in $\gamma_{\max}$ when appropriate. Furthermore, the generalization of the shear rate $\gamma_E = (r/q)\partial(q\nu_{E\times B}/r)/\partial r$ to general geometry[18] $(cRB_\theta/B)d(E_r/B_\theta R)/dr = RB_\theta/B d\Omega/dr$ for pure toroidal rotation at frequency Ω makes it clear that γ_E is not actually a flux surface constant but in fact larger on the outboard side (see Ref. 9 for further discussion). In these illustrations, in keeping with the simple circle $\hat{s}-\alpha$ model, we have treated γ_E as a flux surface average or constant.

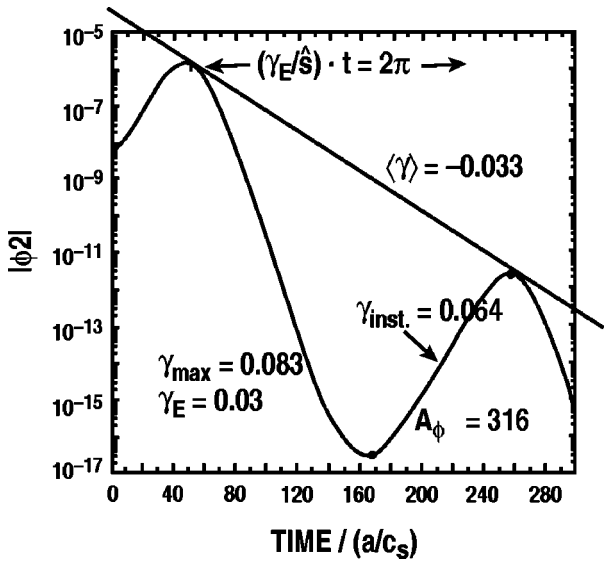

FIG. 1. Linear square amplitude versus time for the most unstable mode ($k_y\rho_s = 0.3$) in the standard case.

Figure 1 illustrates the cyclic nature of the growth rate for the least stable mode in the standard case ($k_y\rho_s = 0.3$) at a relatively weak shear rate of $\gamma_E = 0.03$. $\gamma_{\max} = 0.083$ and the eigenmode or time average rate is $\langle\gamma\rangle = -0.033$ exactly matching the CTW angle average rate $\langle\gamma\rangle_0$. The maximum discernible instantaneous rate is 0.064. Note that during the growing part of the cycle, a large convective amplification 316 is obtained. Figure 2 illustrates the time history of the nonlinear simulation during an initial phase at $\gamma_E = 0$ where the standard case diffusion is 1.9 $[c_s/a\rho_s^2]$, followed by $\gamma_E = 0.03$ where the diffusion level is only slightly depressed despite the fact that all eigenmodes of the system are stable. The finite turbulence results from a nonlinear destabilization. Figure 2 shows a phase in which all amplitudes are instantaneously suppressed by a factor 0.01 yet the diffusion is able to recover. However, if the suppression factor is 0.0001, the turbulence will not recover (not shown in the figure). The only possible interpretation is that the Floquet modes passing though the cycle of convective amplification are able to nonlinearly pump those in the linearly decaying phase if the overall turbulence level is sufficient. We have not verified

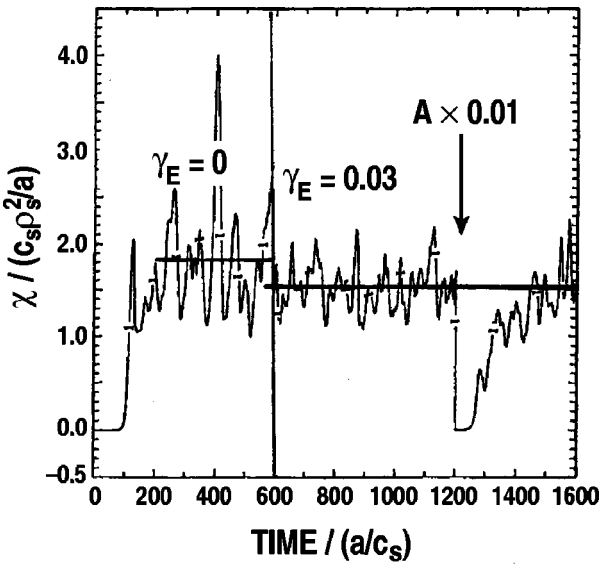

FIG. 2. Time history of the ion diffusivity $\chi/(c_s\rho_s^2/a)$ for the standard case first at $\gamma_E=0$, then at $\gamma_E=0.03$, and finally then multiplying all amplitudes by 1/100.

explicitly, but it seems likely that the critical amplitude level increases with increasing γ_E.

Figure 3 shows how the diffusivity is suppressed then quenches as the γ_E is increased somewhat beyond the maximum ballooning mode growth rate $\gamma_{\max}$. Figure 3(a) shows cases at $a/L_T=3$ and $a/L_T=4$, and Fig. 3(b) shows cases with q variation beyond the standard case at $q=2$. Figure 4 shows how the spectrum of turbulence shifts to the higher wave number k_y as the γ_{E_crit} is approached. Magnetized plasma turbulence always has a spectral peak below the driving wave number ($k_y=0.3$ at $\gamma_E=0$) so that this pattern suggests that the $E\times B$ shear has the strongest effect on lower wave numbers with smaller growth rates.

Perhaps the most interesting and important feature of the $\gamma_{E\_\mathrm{crit}}\approx\gamma_{\max}$ rule is that it appears to hold even to low shear values of magnetic shear $\hat{s}$. Note that γ_E enters the formulation in the combination $\gamma_E/\hat{s}$ so that we might expect that very small $E\times B$ shear levels are required to quench turbulence at vanishing magnetic shear. Indeed, full radius (but not very small ρ_* or high-n) gyrokinetic particle simulation appears to identify $\hat{s}=0$ as a special point in the plasma and the conjectured seat of internal transport barriers.[19] (We hasten to add, however, that other full radius gyrokinetic simulations at smaller ρ_*[20,21] with reverse shear profiles which necessarily have at least some rotational shear, do not show vanishing transport specifically associated with the radial location of $\hat{s}=0$.) From $\rho_*\to 0$, flux tube simulations in the absence of $E\times B$ shear, $\hat{s}=0$ is not a special point for ballooning mode stability or transport.[7,8] There is no support for $\hat{s}=0$ as a special point with $E\times B$ shear in the present simulations. Figure 5 shows a fairly good invariance of the turbulent quenching when the diffusivity normed to diffusivity at $\gamma_E=0$ is plotted versus $\gamma_E/\gamma_{\max}$ from $\hat{s}=0.25$ to 2.0. A corresponding plot versus $(\gamma_E/\hat{s})/\gamma_{\max}$ does not show a good invariance. Note that going to lower $\hat{s}$, the ballooning modes become more extended in θ requiring a larger θ nu-

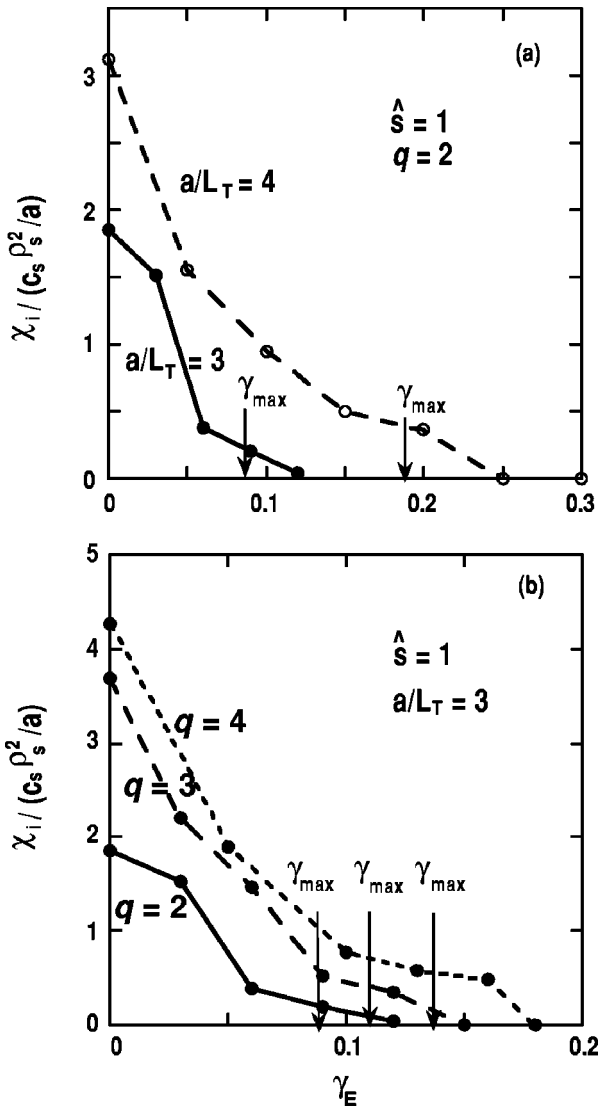

FIG. 3. Ion diffusivity $\chi/(c_s\rho_s^2/a)$ versus γ_E for the standard case at $a/L_T=3$ and at $a/L_T=4$ in (a); and at $q=2$, 3, and 4 for $a/L_T=3$ in (b).

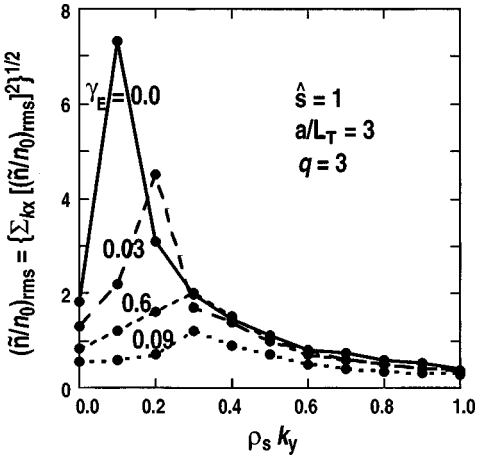

FIG. 4. Spectrum of turbulence $\sqrt{\Sigma_{k_x}(\tilde{n}/n_0)}/(\rho_s/a)$ versus $k_y\rho_s$ at various γ_E for the standard case.

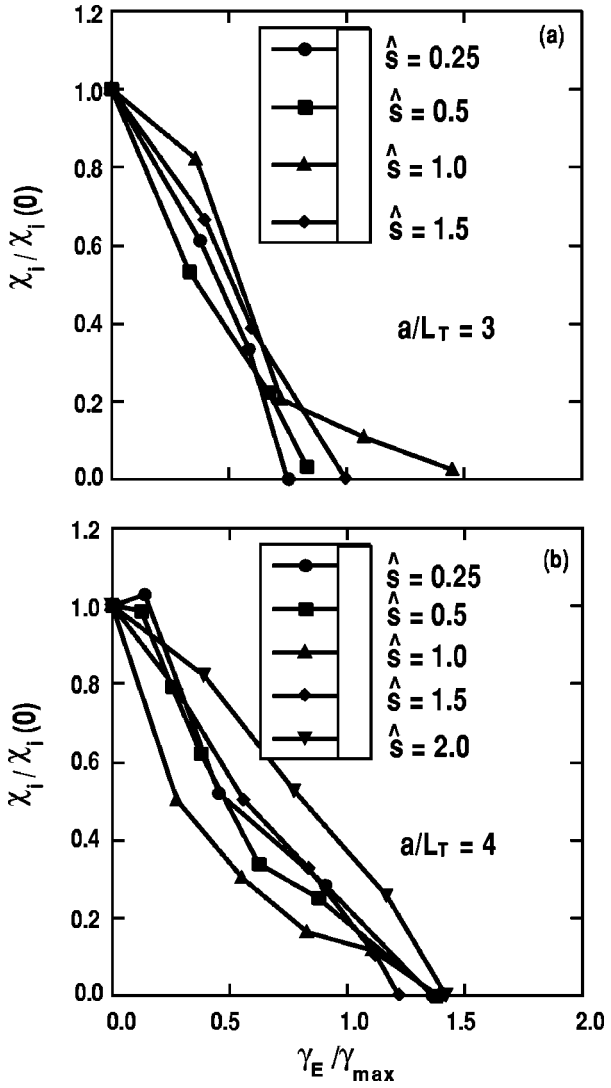

FIG. 5. Ion diffusivity normed to values $\gamma_E=0$, χ/χ_0 versus $\gamma_E/\gamma_{\max}$ at various $\hat{s}$ for the standard case at $a/L_T=3$ in (a) and $a/L_T=4$ in (b).

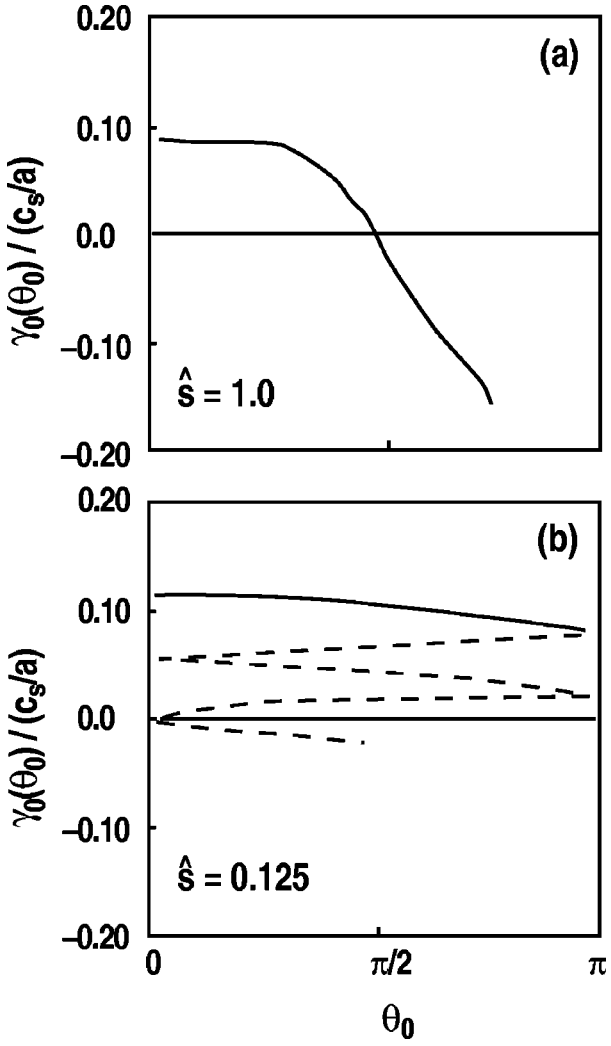

FIG. 6. Linear spectrum of ballooning modes growth rates $\gamma_0(\theta_0)$ versus θ_0 at $\gamma_E=0$ with $k_y\rho_s=0.3$ for the standard case of moderate shear $\hat{s}=1$ in (a) and very low shear $\hat{s}=0.125$ in (b). Dashed lines are schematic of higher harmonics in θ at given θ_0.

merical box. Thus it is too expensive to operate at $\hat{s}$ lower than 0.25 in the Floquet ballooning mode representation [Eq. (2)]. In the ordinary ballooning mode representation [Eq. (1)], we can jump from small $\hat{s}$ to $\hat{s}=0$ even at finite γ_E since the actual grid is in $k_x'=k_y\hat{s}\theta_0$. In the Floquet representation $\hat{s}=0$ implies an infinite rotation speed $\gamma_E/\hat{s}$. The behavior at small $\hat{s}$ can be understood in part by recognizing that at weak γ_E, ballooning modes at the most unstable point θ_0 have to convect farther in θ_0 to reach stability. Figure 6 shows the more unstable mode ($k_y\rho_s=0.3$) spectrum versus θ_0 at $\gamma_E=0$ at moderate [$\hat{s}=1$, Fig. (6a)] and low [$\hat{s}=0.125$, Fig. (6b)]. At small $\hat{s}$, it is better to think of the convection in wave angle $k_x'/k_y=\hat{s}\theta_0$ rather than in θ_0. At small $\hat{s}$, the point of stability is at some invariant value of $k_x'=k_x^*$. At vanishing $\hat{s}$, $\theta_0^*=ky\hat{s}/k_x'^*$ is outside the periodicity points $\theta_0=\pm\pi$, and we must interpret it as modulu 2π. If we estimate $\theta_0^*=\pi/2$ at $\hat{s}=1$, then at $\hat{s}=0.125$, $\theta_0^*=4\pi$ modulu 2π is $\theta_0=0$ which will correspond to a stable higher harmonic in θ modes. [The traceline of harmonics are shown schematically in Fig. 6(b). We cannot see these modes in an initial value code which picks out only the most unstable mode at each θ_0, but from studies of the ideal ballooning mode equations in a k_x' representation, they should be present.] In this way, balancing $(\gamma_E/\hat{s})\partial F/\partial\theta_0$ with $\partial F/\partial t$ in Eq. (1), we obtain $\gamma_{E\_\mathrm{crit}}(k_y/k_x^*)\approx\gamma_{\max}$. The wave angle factor (k_x^*/k_y) is not dissimilar to the wave anisotropy factor $(\Delta k_x/\Delta k_y)$ in the BDT rule.[2] To obtain $\gamma_{E\_\mathrm{crit}}\approx\gamma_{\max}$ invariant to shear, we need only to think of (k_x^*/k_y) $(=\pi/2$ in our example) as $O(1)$ and invariant. Finally, it should be noted that at large $\hat{s}$ (say 1.5), $\gamma_{\max}$ may not occur at $\theta_0=0$.

The critical $E\times B$ shear for eigenmode stability $\gamma_{E\_\langle\gamma\rangle}$ and for poloidal breakup γ_{E_PB} do vanish at vanishing $\hat{s}$. However, Fig. 7 shows very clearly that the critical $E\times B$ shear for quenching turbulence does not follow these linear rates, and in particular eigenmode stability, but is best better described by $\gamma_{E\_\mathrm{crit}}\approx\gamma_{\max}$. The figure also shows that the quench rate does not follow the poloidal breakup rate. We can also define an $E\times B$ shear rate for a given linear convective amplification as the instantaneous linear growth rates

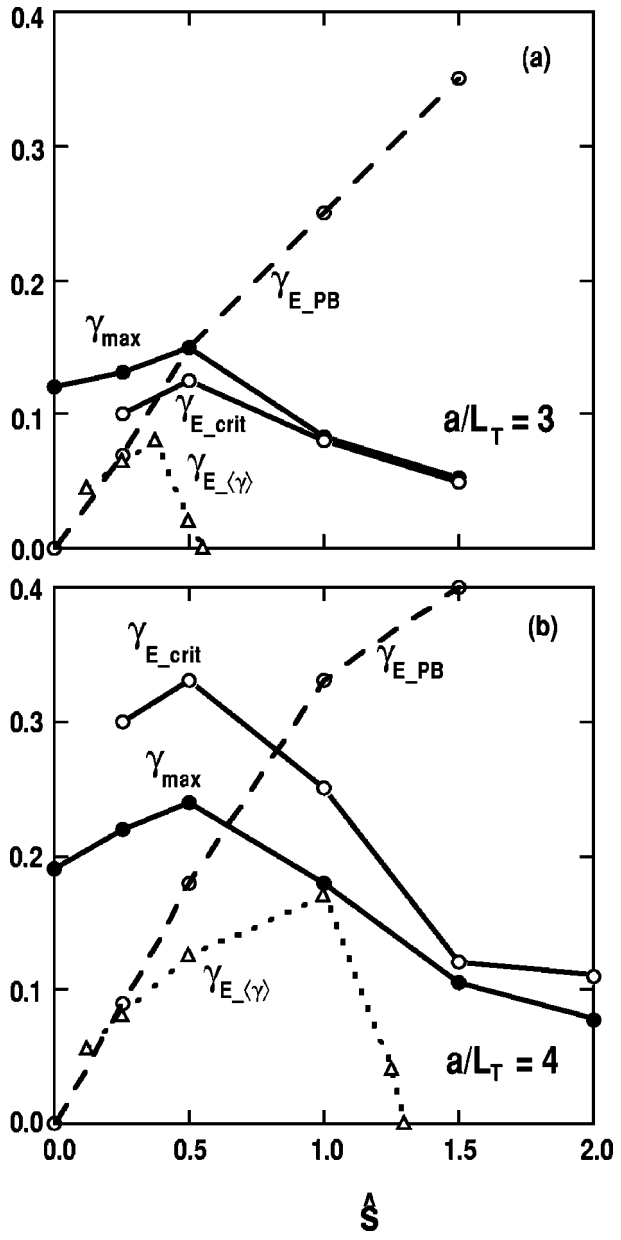

FIG. 7. Comparison of γ_{E_crit}, $\gamma_{E\_\langle\gamma\rangle}$, γ_{E_PB}, and γ_{max} versus shear $\hat{s}$ for the standard case at $a/L_T=3$ in (a) and $a/L_T=4$ in (b).

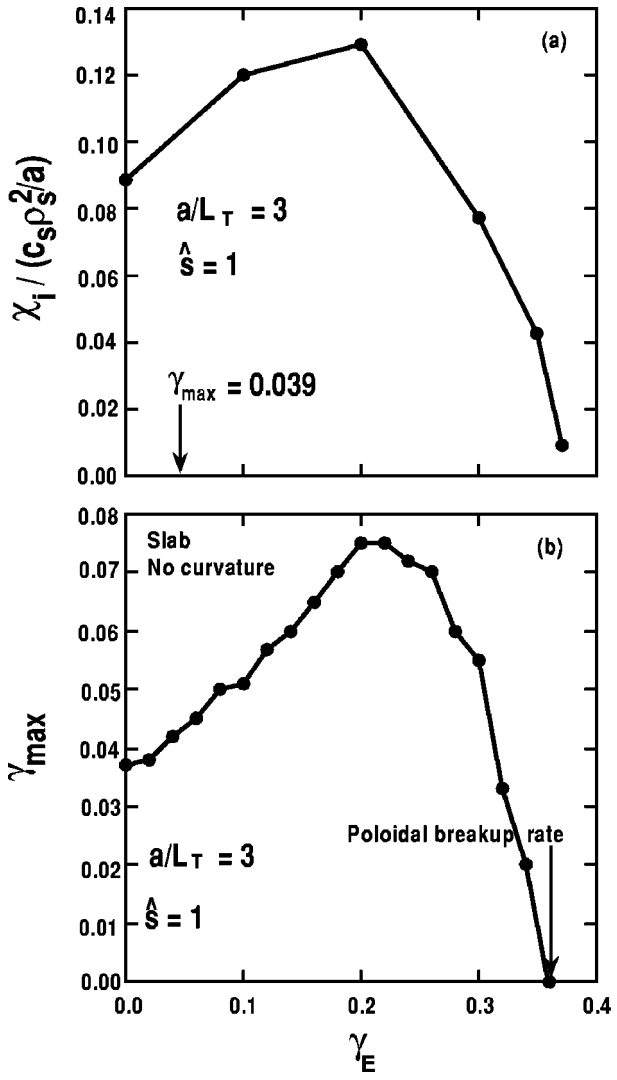

FIG. 8. Ion diffusivity $\chi/(c_s\rho_s^2/a)$ versus γ_E in (a) and γ_{max} versus γ_E in (b) for the slab limit of the standard case.

swing positive on the outboard side. For example, in the $a/L_T=4$ case corresponding to Fig. 7(b), the $E\times B$ rate to limit the amplification to ten-fold in the amplitude (not shown in the figure) is 0.1, 0.17, 0.16, and 0.16 at $\hat{s}=0.5$, 1.0, 1.5, and 2, respectively. While we could associate this fixed amplification rate with the quench rate above from $\hat{s}=1.5-2$ where the eigenmode rate $\gamma_{E\_\langle\gamma\rangle}$ is zero, the quench rate is not generally associated with the fixed amplification rate. The toroidal case is in marked contrast to the slab geometry case where there is no convective amplification process and the quench follows linear eigenmode stability. Rerunning the standard case with no toroidal curvature, Fig. 8(a) shows that the diffusion perfectly tracks the linear eigenmode stability rates versus γ_E shown in Fig. 8(b). This includes not only the destabilizing effect at low γ_E but the

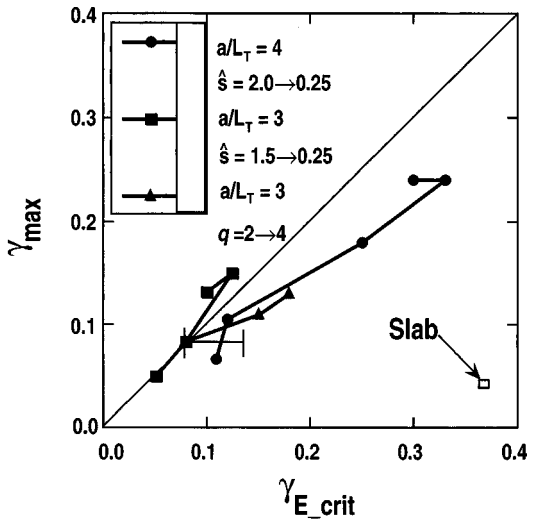

FIG. 9. γ_{max} versus γ_{E_crit} summary of nonlinear simulations.

quench point at $\gamma_{E\_\mathrm{crit}}=\gamma_{E\_\langle\gamma\rangle}=\gamma_{E\_\mathrm{PB}}$ which is more than an order of magnitude larger than $\gamma_{\max}$.

Figure 9 summarizes our results plotting $\gamma_{\max}$ versus γ_{E_crit} suggesting $\gamma_{E\_\mathrm{crit}}=4/3\gamma_{\max}$ with a fidelity of $\pm 30\%$ but only in toroidal geometry. Despite the superficial resemblance of the toroidal quench rule to the BDT[2] rule, the nonlinear two-point renormalization theories, which do not distinguish slab from toroidal geometry, are not well supported qualitatively or quantitatively by these simulations. For these simulations, the normalizing shear rate $\Delta\omega(\Delta k_x/\Delta k_y)$ with $\Delta\omega=D\Delta k_x^2$ (see Ref. 4) does roughly track $\gamma_{\max}$ $[\Delta\omega(\Delta k_x/\Delta k_y)\approx 4\gamma_{\max}]$ in both toroidal and slab geometry, and also roughly tracks $\gamma_{E\text{-crit}}$ $[\Delta\omega(\Delta k_x/\Delta k_y)\approx 3\gamma_{E\_\mathrm{crit}}]$ but only for toroidal geometry. [Note the spectral isotropy factor $(\Delta k_x/\Delta k_y)$ varies by 1.3–2.1 over these simulations.] However, using the suppression formulas of Ref. 4 predicts suppression of only about 10% at the quench point of the toroidal simulations. The suppression formula of Ref. 2 with $\Delta\omega=4D\Delta k_x^2$ appears to be further off.

IV. MODIFICATIONS AND LIMITATIONS ON THE QUENCH RULE FOR GENERAL PROFILE STABILIZATION AT FINITE ρ_*

To assess the likely modifications and limitations on the $\gamma_{E\_\mathrm{crit}}\approx\gamma_{\max}$ rule for physical plasmas and general profile stabilization at finite ρ_*, we examine the linear stability of the ''ballooning-Schrödinger'' dispersion relation.[15]

$$\gamma=\gamma_0+\gamma_0'x+\gamma_0''x^2/2+[\mathrm{Re}(\gamma_0)-\langle\gamma\rangle_0][\cos(\theta_0)-1], \tag{3}$$

for general profile shear $\gamma_0'=d\gamma_0/dx$ and profile curvature $\gamma_0''=d^2\gamma_0/dx^2$. This ansatz results from assuming the variation of the local ballooning mode growth rate $\mathrm{Re}[\gamma_0(r_0,\theta_0)]$ with θ_0 as a $\cos(\theta_0)$ dependence ignoring variation in the frequency. It further assumes the complex rate $\gamma_0(\theta_0,r)$ at $\theta_0=0$ need only be Taylor expanded in $x=r-r_0$ to first (x) and second (x^2) order about the reference radius r_0. The canonical identification $\theta_0=-i\Delta_{ss}d/dx$ $(x=i\Delta_{ss}d/d\theta_0)$, where $\Delta_{ss}=1/\hat{s}k_y$ is the spacing between singular surfaces $(k_y=nq/r)$, is implicit. We look for bound solutions in x space by making the harmonic oscillator expansion for $\theta_0<\pi/2$, $\cos(\theta_0)\to 1-\theta_0^2/2$ followed by $\theta_0=-i\Delta_{ss}(d/dx)$. The third term in Eq. (2) becomes $\gamma_0\Delta k_x^{-2}d^2/dx^2$ where $\Delta k_x=[\gamma_0/\mathrm{Re}(\gamma_0)\xi]^{1/2}k_y\hat{s}$ where $\xi=1-\langle\gamma_0\rangle/\mathrm{Re}(\gamma_0)$. The global wave function is $\Phi=\exp[-(x-x_0)^2/(2\mu^2)]$ where $x_0=(\gamma_0'/\gamma_0'')$ and $\mu=\{\gamma_0/[\Delta k_x^2(-\gamma_0'')]\}^{1/4}$ and the eigenvalue relation is

$$\begin{aligned}\gamma&=\gamma_0-\gamma_{\mathrm{radial}}-\gamma_{\mathrm{shear}}\\&=\gamma_0-1/2(-\gamma_0''\Delta_{ss}^2\xi\gamma_0)^{1/2}-1/2(\gamma_0')^2/\gamma_0''.\end{aligned} \tag{4}$$

The first stabilizing term identified as γ_{radial} corresponds to the familiar $1/n$ ''radial'' profile stabilization. It results entirely from profile curvature γ_0'' and is proportional to ρ_* and typically very small. The boundedness of the global wave function requires $\mathrm{Re}(\gamma_{\mathrm{radial}})/\mathrm{Re}(\gamma_0)>0$. The second stabilizing term identified as γ_{shear} is easily interpreted in the real arithmetic case[15] $[\mathrm{Re}(\gamma_0')=0$ and $\mathrm{Im}(\gamma_0')=0]$ as profile shear stabilization since in the limit of $\rho_*\to 0$ with toroidally driven $E\times B$ shear, $\mathrm{Im}(\gamma_0')/k_y=\gamma_{\mathrm{mode}}\to\gamma_E$. From this we should expect to modify the quench rule by replacing γ_E with $\gamma_{\mathrm{mode}}=(r/q)\partial(q\nu_{\mathrm{mode}}/r)/\partial r$ for finite ρ_*, i.e., we should likely use the shear in the total rotational phase velocity ν_{mode} of the most unstable mode not just its $E\times B$ Doppler shift.

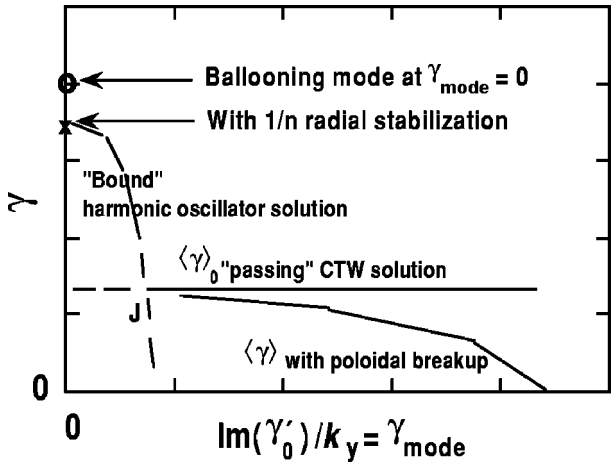

FIG. 10. Illustration of global eigenmode rate versus rotational shear $\gamma_{\mathrm{mode}}/k_y$ in the bound and passing limits.

It is very clear from Eq. (4), however, that finite profile curvature with $\mathrm{Re}(\gamma_0'')<0$ works against profile shear stabilization. We need to ask how much profile shear is required to overcome and ignore profile curvature. This should provide a limitation on the modified quench rule $\gamma_{\mathrm{mode}}\approx\gamma_{\max}$. As the profile shear increases, the harmonic oscillator wave functions acquire an oscillation with decreasing wave number $\langle\langle k_x\rangle\rangle=\mathrm{Im}[\Delta k_x\gamma_0'/(-\gamma_0''\gamma_0)^{1/2}]$. The quarter wavelength of this oscillation must stay less than the spacing between singular surfaces or equivalently $\langle\langle\theta_0\rangle\rangle=\Delta_{ss}\langle\langle k_x\rangle\rangle$ must stay less than $\pi/2$. This harmonic oscillator breakdown point $\langle k_x\rangle\leqslant(\pi/2)/\Delta_{ss}\approx\sqrt{2}/\Delta_{ss}$ is equivalent to $\mathrm{Re}(\gamma_0)-1/2\{\mathrm{Re}[(\gamma_0')/(\gamma_0'')^{1/2}]\}^2\geqslant\langle\gamma\rangle_0$. As the profile shear increases, the growth rate bound (harmonic oscillator) solution decreases until it reaches the growth rate of the passing solution rate which samples all θ_0, i.e., the angle average rate: $\mathrm{Re}(\gamma_0)-1/2\{\mathrm{Re}[(\gamma_0')/(\gamma_0'')]\}=\langle\gamma\rangle_0$ [see Eq. (4) and ignore the small γ_{radial}]. These conditions are very similar and perfectly identical for the real arithmetic case and we use them interchangeably. Figure 10 illustrates the abrupt jump (J) from bound to passing solutions which corresponds to crossing a separatrix[15,16] in the $[x,\theta_0]$ phase space of the ballooning-Schrödinger equation. The passing solutions which do not depend on profile curvature recover the CTW circulation rule rate $\langle\gamma\rangle_0$.[15] (The figure also reminds us that this equation does not include the poloidal breakup effect so that the actual eigenmode rate $\langle\gamma\rangle$ falls below $\langle\gamma\rangle_0$.) Taylor and Wilson[6] argue that when profile curvature is included, the degenerate Floquet modes with their convective amplification are no longer admissible and the eigenmode (a special phased linear combination of Floquet modes) with instantaneous growth rate $\langle\gamma\rangle_0$ must result. Since the quench rule depends on convective amplification of circulating Floquet modes, it seems

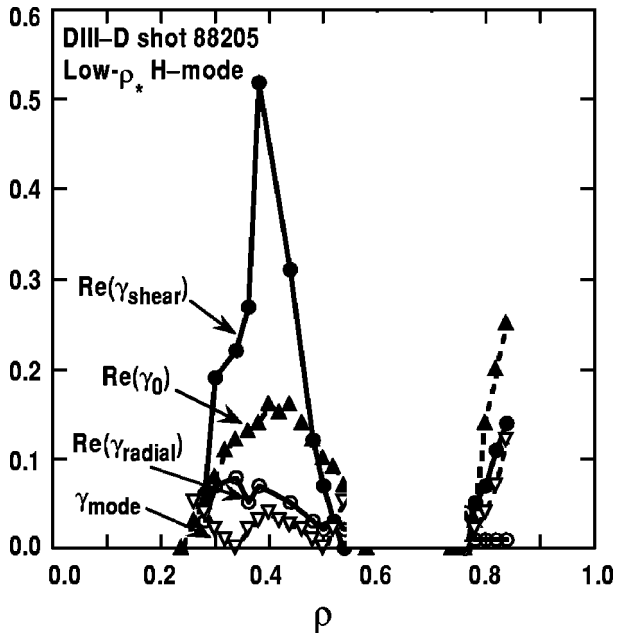

FIG. 11. $\mathrm{Re}(\gamma_0)$, $\mathrm{Re}(\gamma_{\mathrm{radial}})$, $\mathrm{Re}(\gamma_{\mathrm{shear}})$, and γ_{mode} normed to the local c_s/a versus toroidal flux radius ρ for DIII-D H-mode Shot No. 88205 evaluated with the reduced GLF model ballooning mode rates of Ref. 9.

very likely that for the quench rule to be valid, γ_{mode} must be large enough that the jump condition for passing or circulating modes is satisfied. [For completeness, we note that Ref. 22 and also Ref. 20 consider profile bounded eigenmodes in at most the real arithmetic case (and apparently within the harmonic oscillator approximation), but neither reference specifies or clarifies the role of profile curvature $\mathrm{Re}(\gamma_0'')$ or refers to the jump between bound and passing solutions.]

For the real arithmetic case, the jump conditions may be written as $\gamma_{\mathrm{mode}}/\gamma_{\mathrm{max}} > \sqrt{2}/(k_y\rho_s)(\rho_s/L_{\mathrm{curv}})$ beyond which we may ignore curvature $\{1/L_{\mathrm{curv}} = [-\mathrm{Re}(\gamma_0'')/\mathrm{Re}(\gamma_0)]^{1/2}\}$. For small $(\rho_s/L_{\mathrm{curv}})$ of order ρ_* this is safely below $\gamma_{\mathrm{mode}}/\gamma_{\mathrm{max}} \approx 1$ where we expect the quenching rule to apply, i.e., $(\rho_s/L_{\mathrm{curv}}) < (k_y\rho_s)/\sqrt{2} \approx 0.2$. More generally, we expect

$$\gamma_{\mathrm{shear}} = 1/2\{\mathrm{Re}[(\gamma_0')^2/(\gamma_0'')]\} > \mathrm{Re}(\gamma_0) - \langle\gamma\rangle_0, \tag{5a}$$

or interchangeably

$$1/2\{\mathrm{Re}[(\gamma_0')/\gamma_0'']^{1/2}\}^2 > \mathrm{Re}(\gamma_0) - \langle\gamma_0\rangle \tag{5b}$$

is required. In the absence of toroidally driven rotation, this criterion is independent of ρ_*.

As an illustrated application, the dispersion relation Eq. (4) with the ballooning mode rates γ_0 evaluated using a reduced gyrofluid model[9] is shown in Fig. 11. For simplicity, we have assumed $\langle\gamma\rangle_0 \approx 0$, but we stress that it is quite feasible to relax this simplifying assumption using existing gyrokinetic ballooning mode stability codes. The plasma profile is taken from low-ρ_* DIII-D H-mode Shot No. 88205[23] (see Ref. 9 for detailed modeling). The local harmonic oscillator wave functions are well bounded and closely centered to the Taylor expansion point but the harmonic oscillator limit on profile shear is exceeded. In units of local (c_s/a), even though this is a moderately large shear example, γ_{mode} is less than $\gamma_{\mathrm{max}} = \mathrm{Re}(\gamma_0) \gg \mathrm{Re}(\gamma_{\mathrm{radial}})$ but $\mathrm{Re}(\gamma_{\mathrm{shear}})$ exceeds $\mathrm{Re}(\gamma_0)$, i.e., the curvature free criterion (jump condition) Eq. (5) is satisfied at least in the core. However, in the outer core in this example, $\mathrm{Re}(\gamma_{\mathrm{shear}}) \approx \mathrm{Re}(\gamma_0)$ and the criterion is marginal to $\gamma_{\mathrm{mode}} \approx \gamma_{\mathrm{max}}$ and the quench rule is suspect here. Observe also that over some outer portion of the profile where diffusion is clearly turbulent, $\mathrm{Re}(\gamma_0) < 0$ and requires more than a 50% increase in driving temperature gradient to force instability. This behavior is not atypical and likely not due to approximations from the reduced gyrofluid model; more exact linear gyrokinetic studies often have this disconcerting behavior (e.g., Fig. 5 of Ref. 24).

We cannot be confident of these modifications and limitations on the quenching condition for general profiles at finite ρ_* without nonlinear simulations. These cannot be done with the fast flux tube codes and require three-dimensional (3-D) full radius codes which are presently very expensive at physically small ρ_*. When run at too large ρ_*, they are sure to overestimate the profile stabilization effects. Here we report briefly on nonlinear ITG mode simulations with a toroidal two-dimensional (2-D) full radius code.[25] The much faster 2-D codes run with fixed model radial wave functions for the poloidal harmonics. Unfortunately, this means that the 2-D codes cannot include the poloidal breakup effect, and $E\times B$ shear cannot, in general, quench the turbulence unless $\langle\gamma\rangle_0$ is artificially forced to be always less than zero. Preliminary studies of such artificial cases are not inconsistent with the quench rule $\gamma_{\mathrm{mode}} \approx \gamma_{\mathrm{max}}$.

V. SUMMARY

We have developed and applied a novel mode-centered Floquet ballooning mode representation in a flux tube code to simulate ITG turbulence with $E\times B$ rotational shear. This formulation avoids unphysical ''box modes'' of previous simulations. The turbulence quench approximate rule $\gamma_{E\_\mathrm{crit}} \approx \gamma_{\mathrm{max}}$ from the previous simulations[7,8] is recovered. The new formulation makes clear that this quench rule results from a nonlinear convective amplification unique to toroidal geometry. From considerations of the linear Schödinger-ballooning equation,[15] we have suggested that for general finite ρ_* plasmas, the rule should be modified to include the shear in the intrinsic mode velocity and not just the $E\times B$ Doppler shift, i.e., $\gamma_{\mathrm{mode\_crit}} \approx \gamma_{\mathrm{max}}$ where $\gamma_{\mathrm{mode}} = (r/q)\partial(q\nu_{\mathrm{mode}}/r)\partial r$. Furthermore, it is likely that γ_{mode} must be sufficiently large that profile curvature, which could prevent convective amplification, can be ignored. Equation (5) gave criterion for a lower limit on γ_{mode} in terms of the first and second derivatives on the local ballooning mode rates.

ACKNOWLEDGMENTS

We wish to acknowledge many useful discussions with R. L. Miller and G. M. Staebler. R.E.W. thanks The Australian National University, where this work was initiated, for support as a Visiting Fellow.

This is a report of work sponsored by the U.S. Department of Energy under Grant No. DE-FG03-95ER54309 and the Numerical Tokamak Turbulence Project.

[1]K. H. Burrell, Phys. Plasmas **4**, 1499 (1997).
[2]H. Biglari, P. H. Diamond, and P. Terry, Phys. Fluids B **2**, 1 (1990).
[3]K. C. Shaing, E. C. Crume, Jr., and W. Houlberg, Phys. Fluids B **2**, 1492 (1990).
[4]Y. Z. Zhang and S. Mahajan, Phys. Fluids B **2**, 1385 (1992).
[5]J. W. Connor, J. B. Taylor, and H. Wilson, Phys. Rev. Lett. **70**, 1803 (1993).
[6]J. B. Taylor and H. R. Wilson, Plasma Phys. Controlled Fusion **38**, 1999 (1996).
[7]R. E. Waltz, G. D. Kerbel, and J. Milovich, Phys. Plasmas **1**, 2229 (1994).
[8]R. E. Waltz, G. D. Kerbel, J. Milovich, and G. W. Hammett, Phys. Plasmas **2**, 2408 (1995).
[9]R. E. Waltz, G. M. Staebler, W. Dorland, G. W. Hammett, M. Kotschenreuther, and J. A. Konings, Phys. Plasmas **4**, 2482 (1997).
[10]J. W. Connor, R. J. Hastie, and J. B. Taylor, Proc. R. Soc. London, Ser. A **365**, 1 (1979).
[11]W. A. Cooper, Plasma Phys. Controlled Fusion **30**, 1805 (1988).
[12]E. Hameiri and S.-T. Chun, Phys. Rev. A **41**, 1186 (1990).
[13]F. L. Waelbroeck and L. Chen, Phys. Fluids B **3**, 601 (1991).
[14]R. L. Miller and R. E. Waltz, Phys. Plasmas **1**, 2835 (1994).
[15]R. L. Dewar, Plasma Phys. Controlled Fusion **39**, 437 (1997).
[16]F. Rominelli and F. Zonca, Phys. Fluids B **5**, 4082 (1993).
[17]N. Mattor and P. H. Diamond, Phys. Fluids **31**, 1180 (1988).
[18]T. S. Hahm and K. H. Burrell, Phys. Plasmas **1**, 2940 (1990).
[19]Y. Kishimoto, J.-Y. Kim, T. Fukuda, S. Ishida, T. Fujita, T. Tajima, W. Horton, G. Furnish, and M. J. LeBrun, in *Proceedings 16th International Conference on Plasma Physics and Controlled Nuclear Fusion Research, 1996, Montreal, Canada* (International Atomic Energy Agency, Vienna, to be published).
[20]S. E. Parker, H. E. Mynick, M. Artun, J. C. Cummings, V. Decyk, J. V. Kepner, W. W. Lee, and W. M. Tang, Phys. Plasmas **3**, 1959 (1996).
[21]R. D. Sydora, V. K. Decyk, and J. M. Dawson (unpublished).
[22]J. Y. Kim, Y. Kishimoto, M. Wakatani, and T. Tajima, Phys. Plasmas **3**, 3689 (1996).
[23]C. C. Petty, T. C. Luce, K. H. Burrell, S. C. Chiu, J. S. deGrassie, C. B. Forest, P. Gohil, C. M. Greenfield, R. J. Groebner, R. W. Harvey, R. I. Pinsker, R. Prater, and R. E. Waltz, Phys. Plasmas **2**, 2342 (1995).
[24]G. W. Rewoldt, L. L. Lao, and W. M. Tang, Phys. Plasmas **4**, 3293 (1997).
[25]X. Garbet and R. E. Waltz, Phys. Plasmas **3**, 1898 (1996).